Molecular Vision 2020; 26:64-75 <http://www.molvis.org/molvis/v26/64>
Received 25 November 2018 | Accepted 21 February 2020 | Published 24 February 2020

MicroRNA-29b-3p inhibits cell proliferation and angiogenesis by targeting VEGFA and PDGFB in retinal microvascular endothelial cells

Wenyi Tang,[1] Jingli Guo,[1] Ruiping Gu,[1] Boya Lei,[1] Xinyi Ding,[1] Jun Ma,[2,3] Gezhi Xu[1,2,4]

(The first two authors contributed equally to this study.)

[1]Department of Ophthalmology, Eye and ENT Hospital of Fudan University, Shanghai, China; [2]Shanghai Key Laboratory of Visual Impairment and Restoration, Fudan University, Shanghai, China; [3]Research Center, Eye and ENT Hospital of Fudan University, Shanghai, China; [4]NHC Key Laboratory of Myopia (Fudan University); Laboratory of Myopia, Chinese Academy of Medical Sciences, Shanghai, China

Purpose: Excessive angiogenesis, also known as neovascularization, has considerable pathophysiologic roles in several retinal diseases, including retinopathy of prematurity, diabetic retinopathy, and exudative age-related macular degeneration. Accumulated evidence has revealed that miRNAs play important roles in endothelial cell dysfunction and angiogenesis. However, the role of microRNA-29b-3p (miR-29b-3p) in retinal angiogenesis is still unclear. Therefore, we investigated whether and how miR-29b-3p affects the function of retinal microvascular endothelial cells (RMECs).
Methods: The overexpression and inhibition of miR-29b-3p were achieved by transfecting rat RMECs with an miR-29b-3p mimic and inhibitor, respectively. The proliferation, migration, and angiogenesis of RMECs were evaluated using a Cell Counting Kit-8 assay, Ki67 staining, western blotting (of proliferating cell nuclear antigen, cyclin A2, cyclin D1, and cyclin E1), wound healing test, and tube formation assay. The expression levels of vascular endothelial growth factor A (VEGFA) and platelet-derived growth factor B (PDGFB) were examined with quantitative real-time PCR and western blotting, respectively.
Results: Overexpression of miR-29b-3p statistically significantly inhibited the function of RMECs in cell proliferation and angiogenesis, while inhibition of miR-29b-3p increased the proliferative and angiogenic activities of RMECs. Moreover, VEGFA and PDGFB, as the targets of miR-29b-3p, were statistically significantly downregulated by the miR-29b mimic, whereas the miR-29b-3p inhibitor had the opposite effects.
Conclusions: miR-29b-3p negatively regulates RMEC proliferation and angiogenesis, at least partly by targeting VEGFA and PDGFB. These data may provide a potential therapeutic strategy for treating ocular neovascular diseases.

Abnormal development of blood vessels within the retina (retinal neovascularization) plays important roles in many ocular neovascular diseases, including retinopathy of prematurity, proliferative diabetic retinopathy, and wet age-related macular degeneration [1]. Endothelial cell proliferation and migration lead to the angiogenic growth of new blood vessels sprouting from retinal veins, and may result in vitreous hemorrhage, retinal detachment, and even blindness [2]. Previous studies have shown that retinal angiogenesis is regulated by many angiogenesis-related factors, including vascular endothelial growth factor (VEGF), platelet-derived growth factor (PDGF), fibroblast growth factor (FGF), and transforming growth factor [3]. Currently, the main treatment for retinal neovascularization involves intravitreal injection of anti-VEGF agents, such as ranibizumab and bevacizumab. However, some patients show poor or no response to anti-VEGF agents with limited or no visual improvement [4], suggesting that other molecules (e.g., PDGF and basic FGF) may be involved in retinal neovascularization [5,6]. Considering that neovascularization involves a complex orchestra of activities with a broad network of growth factors, a monotherapeutic approach with an anti-VEGF agent may result in incomplete or ineffective treatment. Thus, the development of alternative therapies that target multiple components of the angiogenic pathway is imperative.

MicroRNA (miRNAs) are small (18–25 nucleotides long), endogenously expressed non-coding RNAs. They modulate biologic processes at the post-transcriptional level by binding to the 3′-untranslated region (3′-UTR) of their target genes, leading to translational repression or degradation [7,8]. In recent years, miRNAs have been shown to be involved in various biologic processes, including proliferation, differentiation, development, and metabolism, as well as in various diseases [9]. miRNAs also play pivotal roles in regulating

Correspondence to: Gezhi Xu, Department of Ophthalmology, Eye and ENT Hospital of Fudan University, 83 Fen Yang Road, Shanghai, 200031, China; Phone: +86 021 64377134; FAX: +86 021 64377151; email: xugezhi@sohu.com

endothelial function and angiogenesis in the retina [10,11]. miR-29b is a member of the miR-29 family, which includes three highly conserved mature miR-29s (miR-29a, miR-29b, and miR-29c) [12]. Recent studies indicate that miR-29b is a multifunctional miRNA participating in various pathologies, including muscle atrophy [13], tissue fibrosis [14], metabolic disorders [15], and cancers, such as endometrial carcinoma [16], breast cancer [17], and glioblastoma [18]. In particular, it was reported that miR-29b can regulate cell proliferation, differentiation, migration, and invasion of cancer cells, and participate in tumor angiogenesis [19]. However, the effects of miR-29b on retinal microvascular endothelial cell biology have not been reported yet.

In the present study, we investigated the roles of miR-29b-3p, as the leading strand of miR-29b, in retinal microvascular endothelial cells (RMECs). The results show that miR-29b-3p inhibits RMEC proliferation and angiogenesis, at least in part by targeting VEGFA and PDGFB.

METHODS

Cell culture: Rat primary RMECs were purchased from Cell Biologics Company (Chicago, IL; catalog no. RA-6065), and the certificate of analysis is listed in Appendix 1. RMECs were grown on cell culture flasks in endothelial cell medium (catalog no. 22,956; ScienCell, Carlsbad, CA) supplemented with 5% fetal bovine serum (catalog no. 0025; ScienCell), 100 units/ml penicillin and 100 µg/ml streptomycin (catalog no. 0503; ScienCell), and 1% endothelial cell growth supplement (catalog no. 1052; ScienCell). Cells between passages 4 and 10 were used in all experiments to maintain the primary characteristics of endothelial cells.

Cell groups and transfection: RMECs were plated on six-well plates, 1 day before transfection. At about 50–60% confluence, the cells were transfected with the miR-29b-3p mimic (miR-29b-3p-mimic), mimic negative control (NC mimic), miR-29b-3p inhibitor (anti-miR-29b-3p), or anti-negative control (anti-NC) synthesized by Ribobio (Guangzhou, China) at a final concentration of 100 nmol/l using Lipofectamine 3000 transfection reagent (Life Technologies, Carlsbad, CA) according to the manufacturer's protocols. A mock transfection group received only the transfection reagents.

Cell viability assay: Cell viability was assessed using Cell Counting Kit-8 (CCK-8, Dojindo, Kumamoto, Japan) assays according to the manufacturer's instructions. RMECs (3×10^3 cells/well) were seeded on 96-well plates and incubated at 37 °C in 5% CO_2 overnight, and then transfected with NC mimic, miR-29b-3p-mimic, NC inhibitor, or anti-miR-29b-3p. After incubation for 48 h, 10 µl CCK-8 solution was added to each well, and the wells were incubated for another 2 h at 37 °C. Absorbance was measured at 450 nm using a spectrophotometer (Thermo Scientific, Rockford, IL).

Wound scratch assays: Cells were seeded on six-well plates and transfected with NC mimic, miR-29b-3p-mimic, anti-NC, or anti-miR-29b-3p until they were 90% confluent. A sterile 200 µl pipette tip was used to scratch a wound in the cell monolayer, and then the wells were washed with cold PBS (1X; 155 mM NaCl, 3 mM Na_2HPO_4-$7H_2O$, 1 mM KH_2PO_4, pH 7.4; Gibco, Grand Island, NY) twice. The cells were then grown in fresh medium, and the wounds in each well were photographed at 0 and 6 h under a light microscope (Leica Microsystems, Wetzlar, Hesse-Darmstadt, Germany). The scratch width in each image was measured using ImageJ software (ImageJ). The wound healing rate was calculated as follows: wound healing rate = (initial scratch width − final scratch width) / initial scratch width × 100%.

Tube formation assay: In vitro: Angiogenesis was assessed with the tube formation ability on Matrigel (BD Biosciences, Franklin Lakes, NJ). Briefly, 50 µl/well of Matrigel diluted in serum-free medium (1:1) was added to 96-well plates and incubated at 37 °C for 30 min. Transfected cells (1×10^4 cells/well) were seeded on the Matrigel-coated wells and incubated at 37 °C for 6 h. Tube formation was assessed on photographs taken with a light microscope (Leica Microsystems). The total tube length in each image was quantified using ImageJ software.

Immunofluorescence: Cells were grown on coverslips in 24-well plates and fixed in 4% paraformaldehyde for 15 min at room temperature. After washing three times in PBS, the cells were blocked with 5% fetal bovine serum for 1 h at room temperature. The cells were then incubated with primary anti-CD31 antibody (1:100, AF3628; R&D Systems, Minneapolis, MN) or anti-Ki67 antibody (1:100, ab15580; Abcam, Cambridge, UK) overnight at 4 °C. After washing three times with PBS, the cells were incubated with corresponding secondary antibodies (1:1000; Invitrogen, Carlsbad, CA) for 1 h at room temperature. The cells were rinsed with PBS and incubated with 4′,6-diamidino-2-phenylindole (Yeasen Biotech, Shanghai, China) for 5 min. After mounting with glycerol, the coverslips were analyzed with fluorescence microscopy (Leica Microsystems).

Quantitative real-time PCR: At 48 h after transfection, total RNA was extracted from the cultured cells using TRIzol reagent (Invitrogen) according to the manufacturer's instructions. For miRNA expression analysis, miRNA was reverse-transcribed using specific real-time (RT) primers (Ribobio) at 42 °C for 60 min and 70 °C for 10 min. Quantitative real-time PCR reactions were performed using the Bulge-Loop™ miRNA qRT-PCR Starter Kit (miR-29b-3p

Product ID: MQP-0101; U6 Product ID: MQP-0201; Ribobio) according to the manufacturer's protocols. A SYBR Green PCR system (Applied Biosystems, Foster City, CA) was used under the following conditions: 95 °C for 10 min, followed by 40 cycles at 95 °C for 2 s, 60 °C for 20 s, and 70 °C for 10 s. To assess VEGFA and PDGFB mRNA expression, we used the following primers: VEGFA forward 5′-AAA GCC CAT GAA GTG GTG AAG-3′, reverse 5′-CAT CTC TCC TAT GTG CTG GCT TT-3′; PDGFB forward 5′-CGC TAA CAT CAA ATG GGG TG-3′, reverse 5′-TTG CTG ACA ATC TTG AGG GAG-3′; GAPDH forward 5′-CGC TAA CAT CAA ATG GG GTG-3′, reverse 5′-TTG CTG ACA ATC TTG AGG GAG-3′; all primers were synthesized by Genecreate (Wuhan, China). cDNAs (cDNAs) were synthesized using the M-MLV Reverse Transcriptase Kit (ELK Biotechnology, Wuhan, China) with the following conditions: 42 °C for 60 min, 85 °C for 5 min, and hold at 4 °C. Real-time PCR was performed using a StepOne™ Real-Time PCR instrument (Thermo Scientific) The thermal cycling conditions were 95 °C for 1 min, followed by 40 cycles of 95 °C for 15 s, 58 °C for 20 s, and 72 °C for 45 s, and the melting curve profiles were generated at the end. Glyceraldehyde 3-phosphate dehydrogenase (GAPDH) and U6 were used as loading controls to quantify the mRNA and miRNA expression levels, respectively, using the formula: $2^{-\Delta\Delta Ct}$.

Western blotting: At 72 h after transfection, cells were harvested with 0.05% Trypsin-EDTA (Thermo Scientific), washed with PBS, and lysed with radioimmunoprecipitation assay (RIPA) buffer (Beyotime, Jiangsu, China). The protein concentration was measured using a BCA Protein Assay kit (Beyotime). Equal amounts of protein (30 μg) were loaded and separated on 12% sodium dodecyl sulfate–polyacrylamide gels. Then, the gels were transferred to polyvinylidene difluoride membranes (Millipore, Billerica, MA). After blocking for 1 h in 5% skimmed milk at room temperature, the membranes were incubated overnight at 4 °C with antibodies for proliferating cell nuclear antigen (PCNA; 1:1,000; sc-25280; Santa Cruz Biotechnology, Dallas, TX), cyclin A2 (1:1,000; ab38; Abcam), cyclin E1 (1:1,000; 20808s; Cell Signaling Technology, Danvers, MA), cyclin D1 (1:1,000; ab134175; Abcam), VEGFA (1:1,000; 19,003-1-AP; Proteintech Group, Chicago, IL), PDGFB (1:1,000; ab178409; Abcam), and β-tubulin (1:1,000; AB0039; Abways, Shanghai, China). After incubation with corresponding horseradish-peroxidase-conjugated secondary antibodies for 1 h at room temperature, the blots were visualized with Super Enhanced Chemiluminescence (ECL) Detection Reagent (Yeasen Biotech), and the signals were analyzed using ImageJ software. Full western blots are shown in Appendix 2, Appendix 3, Appendix 4, Appendix 5, Appendix 6, Appendix 7, Appendix 8, and Appendix 9.

Statistical analysis: All experiments were repeated independently at least three times. Data are expressed as the mean ± standard deviation. One-way ANOVA followed by Tukey's multiple comparisons test was used for all statistical analyses. Statistical significance was defined as a p value of less than 0.05. Statistical analyses were performed using GraphPad Prism 5.0 (GraphPad, San Diego, CA).

RESULTS

Overexpression of miR-29b-3p inhibited RMEC proliferation: The cultured RMECs were fusiform-shaped, and showed abundant expression of CD31, a biomarker for endothelial cells (Figure 1). To elucidate the specific role of miR-29b-3p in the angiogenic response of endothelial cells, RMECs were first transiently transfected with miR-29b-3p-mimic. Quantitative real-time PCR revealed that the expression of miR-29b-3p was dramatically improved by miR-29b-3p-mimic transfection compared with that of the NC group (Figure 2A). We then examined the effects of miR-29b-3p on cell proliferation in RMECs. The results of the CCK-8 assay showed that miR-29b-3p overexpression statistically significantly decreased the viability of RMECs compared with that of the NC group at 48 h post-transfection (Figure 2B). Ki67 staining and PCNA expression, both of which are commonly used as markers of cell proliferation [20], were detected in the RMECs. We found that miR-29b-3p overexpression statistically significantly reduced the percentage of Ki67-positive RMECs and inhibited PCNA protein expression compared with those of the NC group (Figure 2C–F). We also examined the expression levels of the cell cycle–related proteins cyclins A2, D1, and E1 to determine whether miR-29b-3p regulates cell cycle progression in RMECs. Western blotting revealed that miR-29b-3p transfection decreased the expression levels of these cyclins compared with those of the NC group (Figure 2G–J). Taken together, these results suggested that miR-29b-3p overexpression suppressed cell proliferation and cell cycle progression of RMECs in vitro.

miR-29b-3p overexpression attenuated RMEC angiogenesis: To determine the roles of miR-29b in RMEC angiogenesis, we performed wound scratch and tube formation assays. The results of these assays indicate that the RMECs treated with miR-29b-3p moved slower than the NC-transfected cells at 6 h post-transfection (Figure 3A,B). As shown in Figure 3C,D, the total tube length was statistically significantly smaller in the miR-29b-3p-mimic group than in the NC group at 6 h post-transfection (Figure 3C,D). There were no apparent differences in the wound healing rates or total tube lengths between the mock and NC groups. These results indicated

that miR-29b-3p overexpression inhibited RMEC angiogenesis in vitro.

Inhibition of miR-29b-3p enhanced RMEC proliferation: After establishing the effects of miR-29b-3p overexpression on RMECs, we next transfected cells with anti-miR-29b-3p to inhibit miR-29b-3p. Quantitative real-time PCR confirmed that anti-miR-29b-3p transfection statistically significantly inhibited miR-29b-3p expression (Figure 4A). Then, we examined the effects of anti-miR-29b-3p on RMEC proliferation. As shown in Figure 4B, anti-NC did not statistically significantly affect cell viability, whereas anti-miR-29b-3p statistically significantly increased RMEC viability compared with that of the anti-NC group at 48 h post-transfection (Figure 4B). Ki67 staining and western blotting revealed that anti-miR-29b-3p transfection resulted in more Ki67-labeled cells and increased PCNA protein expression compared with those of the anti-NC group (Figure 4C–F). Additionally, the protein expression levels of cyclin A2, cyclin D1, and cyclin E1 in the RMECs were statistically significantly elevated by anti-miR-29b-3p transfection compared with those of the anti-NC group at 72 h post-transfection (Figure 4G–J). These observations suggest that inhibition of miR-29b-3p enhances cell proliferation and cell cycle progression of RMECs in vitro.

Inhibition of miR-29b-3p facilitated RMEC angiogenesis: We also examined the effects of anti-miR-29b-3p on cell migration and tube formation. The wound scratch test showed that inhibition of miR-29b-3p accelerated RMEC migration at 6 h post-transfection compared with that of the anti-NC group (Figure 5A,B). Moreover, inhibition of miR-29b-3p increased the total tube length of the RMECs compared with that of the anti-NC group at 6 h post-transfection (Figure 5C,D). There were no apparent differences in the wound healing rates or total tube lengths between the mock and anti-NC groups. Overall, these data indicate that miR-29b-3p acts as a negative regulator of RMEC angiogenesis.

miR-29b-3p negatively regulated the expression of angiogenic factors in RMECs: Previous studies showed that VEGFA and PDGFB are regulators of the proliferation and vessel growth of endothelial cells [21, 22]. MiR-29b has been demonstrated to bind to the 3′-UTR of VEGFA and PDGFB in 293T cells and other types of cells, by using the dual luciferase reporter gene assays [17, 23–26]. Therefore, we examined whether these growth factors are involved in the antiangiogenic effects of miR-29b in RMECs. As shown in Figure 6A, bioinformatic analysis using miRDB showed that the miR-29b-3p recognition sites on the 3′-UTR sequences of VEGFA and PDGFB are highly conserved among vertebrates, including rats, humans, and mice. Moreover, we performed quantitative real-time PCR and western blotting to determine the effects of miR-29b-3p on the gene and protein expression levels of VEGFA and PDGFB in RMECs. Compared with the RMECs transfected with NC, the mRNA levels of VEGFA and PDGFB were statistically significantly reduced by miR-29b-3p (Figure 6B,C). Likewise, western blotting revealed that transfection with miR-29b-3p-mimic noticeably reduced the protein expression levels of VEGFA and PDGFB (Figure 6D–G). In contrast, downregulation of miR-29b-3p statistically significantly increased the mRNA (Figure 6H,I) and protein (Figure 6J–M) expression levels of VEGFA and PDGFB compared with those of the NC group. These results indicate that miR-29b-3p regulates cell proliferation and angiogenesis, at least in part by targeting VEGFA and PDGFB.

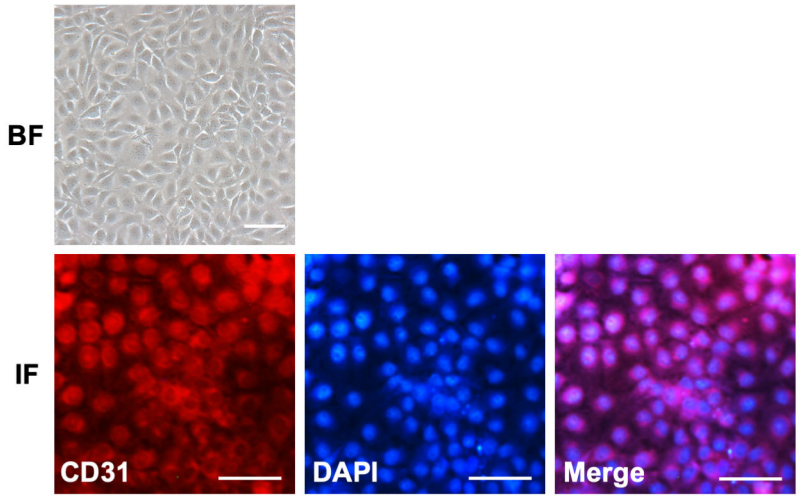

Figure 1. Characterization of rat primary RMECs. Light microscopic bright-field (BF) images showing the fusiform shape of retinal microvascular endothelial cells (RMECs). Immunofluorescence (IF) of CD31-labeled RMECs. The endothelial cell marker CD31 was primarily expressed on the cell membrane. 4′,6-diamidino-2-phenylindole (DAPI) was used to label cell nuclei. Scar bar: 50 µm.

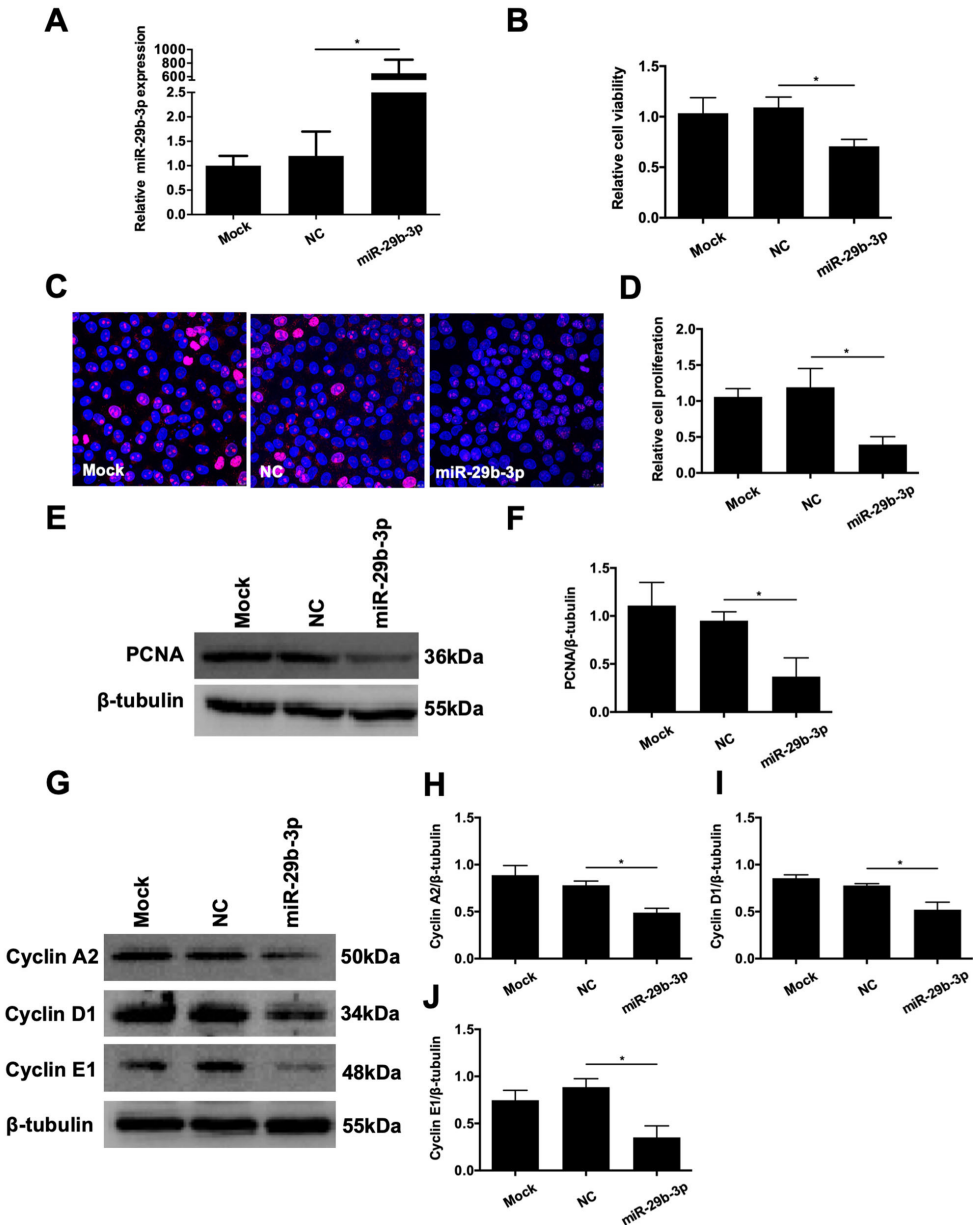

Figure 2. Effects of microRNA (miR)-29b-3p on the proliferation of RMECs. **A**: Retinal microvascular endothelial cells (RMECs) were transiently transfected with 100 nmol/l of miR-29b-3p mimic (miR-29b-3p-mimic) or negative control (NC) mimic. Quantitative real-time PCR confirmed that the expression of miR-29b-3p was increased in the miR-29b-3p-mimic group compared with that of the NC group. **B**: At 48 h after transfection, cell viability was assessed with Cell Counting Kit-8 (CCK-8) assays, and relative cell viability was calculated against the mock-transfected cells. RMECs transfected with miR-29b-3p-mimic showed statistically significantly decreased cell viability compared with that of the NC group. **C**, **D**: At 48 h after transfection, immunofluorescent staining of Ki67 revealed that the proportion of Ki67-positive cells was decreased by transfection with miR-29b-3p-mimic compared with that of the NC group. The relative cell proliferation rate was calculated against mock-transfected cells. **E**, **F**: At 72 h after transfection, western blotting showed that the protein expression of proliferating cell nuclear antigen (PCNA) was statistically significantly decreased by miR-29b-3p-mimic compared that of with the NC group. **G**–**J**: At 72 h after transfection, western blotting showed that the protein expression levels of cyclin A2, cyclin D1, and cyclin E1 were statistically significantly downregulated by miR-29b-3p-mimic compared those of with the NC group. U6 and β-tubulin were used as the internal controls for miR-29b-3p expression and western blotting, respectively. n=3 per group. *p<0.05.

DISCUSSION

In the present study, we found that overexpression of miR-29b-3p inhibited endothelial proliferation and angiogenesis of RMECs, whereas miR-29b-3p inhibition had the opposite effects. These effects of miR-29b-3p on RMECs were mediated by negatively regulation of VEGFA and PDGFB expression. To the best of our knowledge, this is the first study to demonstrate the effects of miR-29b on cell proliferation and angiogenesis of RMECs.

Recent studies have provided statistically significant insight into the biology and clinical relevance of the miR-29 family, which comprises miR-29a, miR-29b-1, miR-29b-2, and miR-29c. Mature miR-29s are highly conserved across humans, rats, and mice. The sequences of mature miR-29b-1 and miR-29b-2 are identical, and they are referred to as miR-29b. miR-29b is an important regulator of many cellular processes, including cell proliferation, differentiation, and apoptosis [12]. Previous studies revealed that miR-29b acts

as a tumor suppressor in many tumor types, and downregulation of miR-29b has been linked with many types of cancer, including acute myelogenous leukemia [27], invasive breast cancer [28], lung cancer [29], and cholangiocarcinoma [30]. It was reported that the induction of miR-29b expression led to reduced cell growth and the induction of apoptosis in myeloid leukemia cell lines by regulating apoptosis, cell cycle, and proliferation [27]. Moreover, Fabbri et al. reported that the miR-29 family could inhibit tumor growth by suppressing DNA methyltransferase and normalizing aberrant methylation in lung cancer cell lines [31]. It was also reported that miR-29 overexpression inhibited the proliferation of esophageal squamous cell carcinoma cells, and induced cell cycle arrest at the G0–G1 stage by suppressing cyclin E expression [32]. However, the roles of miR-29b in ocular diseases, especially retinal neovascularization, remain largely unknown. In the present study, we found that miR-29b-3p inhibited endothelial cell proliferation. Meanwhile, the expression of PCNA, a marker for cell proliferation, was also inhibited by miR-29b-3p. The cyclins D1, E1, and A2 are key proteins implicated in the G0–G1 and G1–S transitions, which permit cells to enter the S phase of the cell cycle and promote cell proliferation [33-35]. We found that miR-29b-3p downregulated the expression levels of cyclins A2, D1, and E1, which indicates that it inhibited cell cycle progression and proliferation of RMECs. In contrast, inhibition of miR-29b-3p had the opposite effects. These results indicate that miR-29b acts as a negative regulator of cell cycle progression and proliferation of RMECs.

Another important function of the miR-29 family is regulation of the extracellular matrix [12]. It has been shown that miR-29s target up to 16 extracellular matrix genes implicated in fibrosis in many organs and tissues [12]. Loss of regulation of extracellular matrix by miR-29s may also facilitate cell migration. For example, Chou et al. reported that miR-29b suppressed breast cancer migration

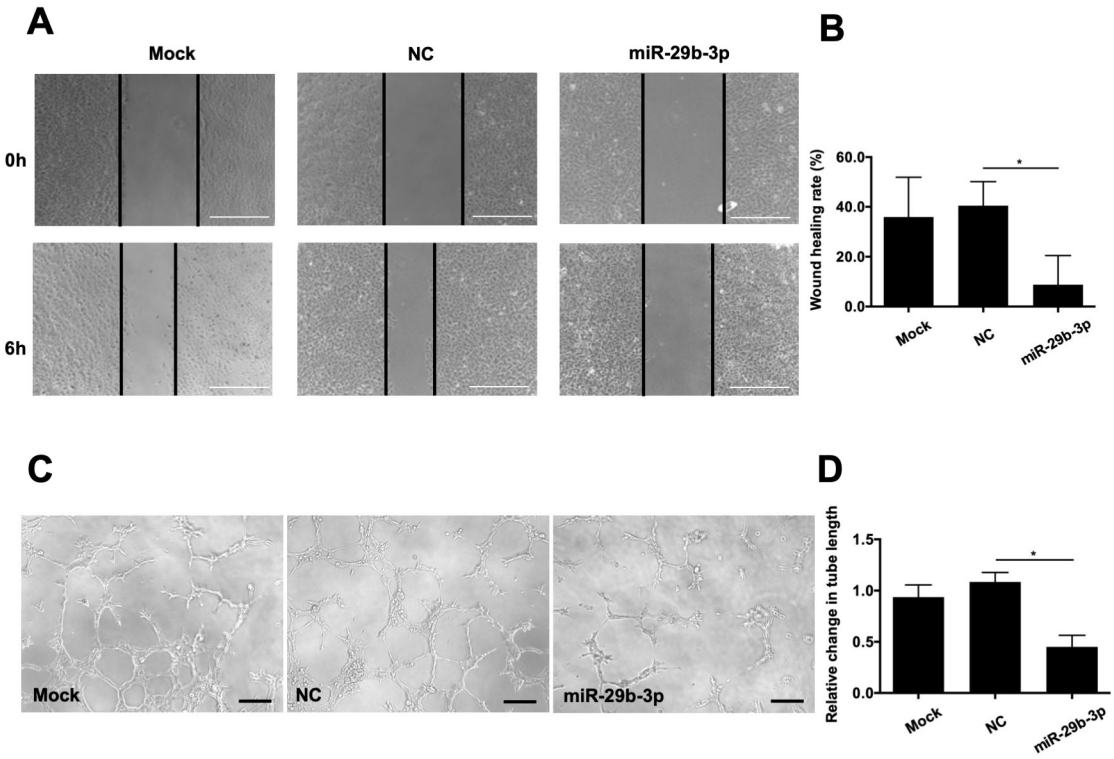

Figure 3. Effects of microRNA (miR)-29b-3p on the migration and angiogenesis of RMECs. **A**: Representative images of wound scratch assays after transfecting retinal microvascular endothelial cells (RMECs) with 100 nmol/l of miR-29b-3p-mimic or negative control (NC) mimic. Images were taken at 0 and 6 h after the cell layer was scratched with a pipette tip. Scale bar: 500 µm. **B**: Statistical analysis of the wound healing rates revealed that transfection with miR-29b-3p-mimic statistically significantly inhibited RMEC migration compared that of with the NC group. **C**: Representative images of tube formation assays at 6 h after seeding RMECs transfected with 100 nmol/l of miR-29b-3p or NC on Matrigel. Scale bar: 100 µm. **D**: Statistical analysis of the relative change in tube length revealed that transection with miR-29b-3p-mimic statistically significantly inhibited tube formation in RMECs compared with that of the NC group. Tube length was quantified by calculating the cumulative length of the tubes in each image, and the relative change was compared against the mock-transfected group. n=3 per group. *p<0.05.

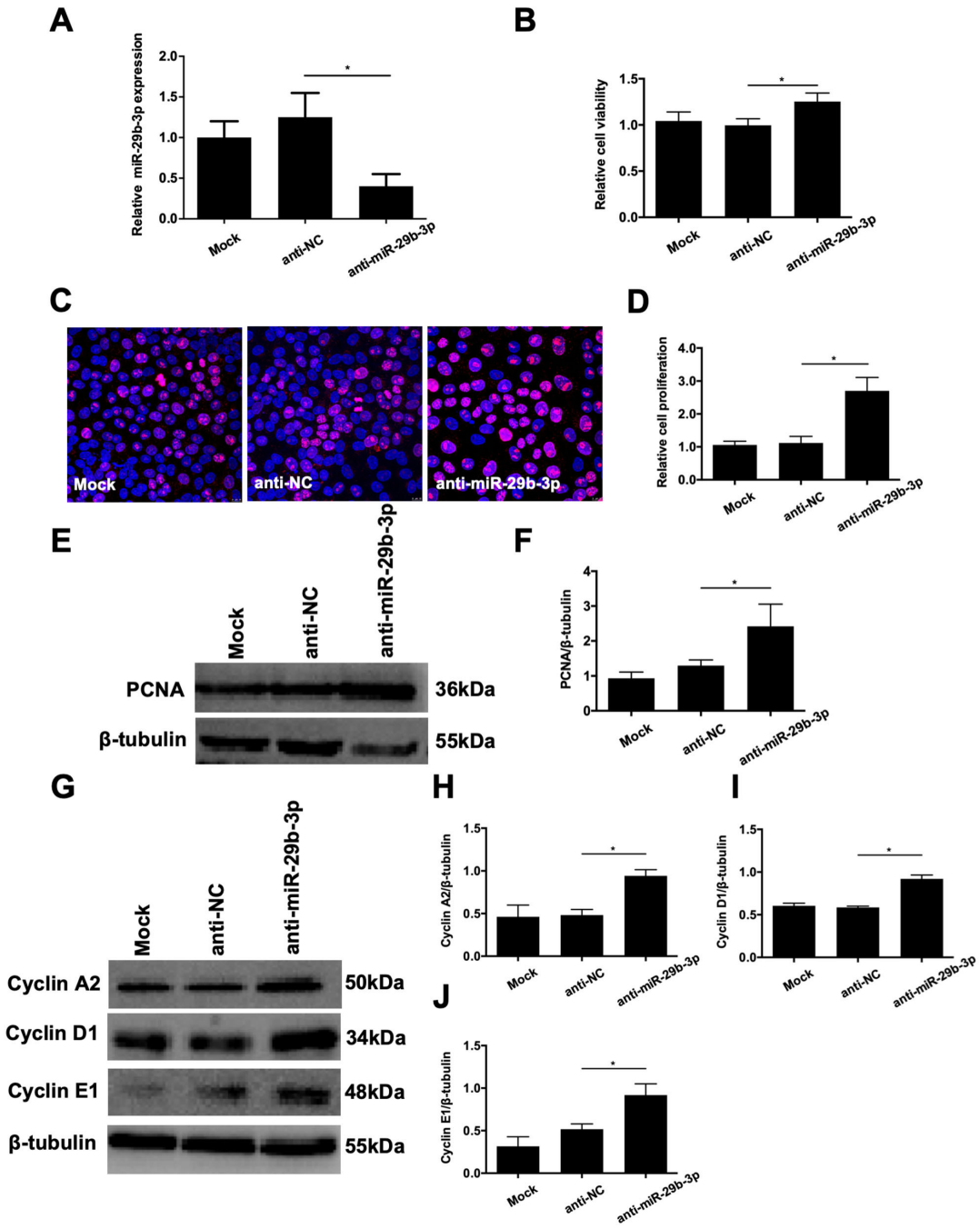

Figure 4. Effects of anti-microRNA (miR)-29b-3p on the proliferation of RMECs. **A**: Retinal microvascular endothelial cells (RMECs) were transfected with 100 nmol/l of anti-miR-29b-3p or negative control inhibitor (anti-NC). Quantitative real-time PCR confirmed that transfection with anti-miR-29b-3p decreased the expression level of miR-29b-3p compared with that of the anti-NC group. **B**: At 48 h after transfection, cell viability was assessed using CCK-8 assays, and relative cell viability was calculated against mock-transfected cells. Transfection with anti-miR-29b-3p statistically significantly increased the viability of RMECs compared with that of the anti-NC group. **C**, **D**: At 48 h after transfection, immunofluorescent staining showed that transfection with anti-miR-29b-3p increased the proportion of Ki67-labeled cells compared with that of the anti-NC group. The relative proliferation rate of RMECs determined by Ki67 staining was calculated against mock-transfected cells. **E**, **F**: At 72 h after transfection, western blotting showed that the protein expression of proliferating cell nuclear antigen (PCNA) was statistically significantly increased by anti-miR-29b-3p compared with that of the NC group. **G**–**J**: At 72 h after transfection, western botting showed that the protein expression levels of cyclin A2, cyclin D1, and cyclin E1 were statistically significantly upregulated by anti-miR-29b-3p compared with those of the anti-NC group. U6 and β-tubulin were used as the internal controls for miR-29b-3p expression and western blotting, respectively. n=3 per group. *p<0.05.

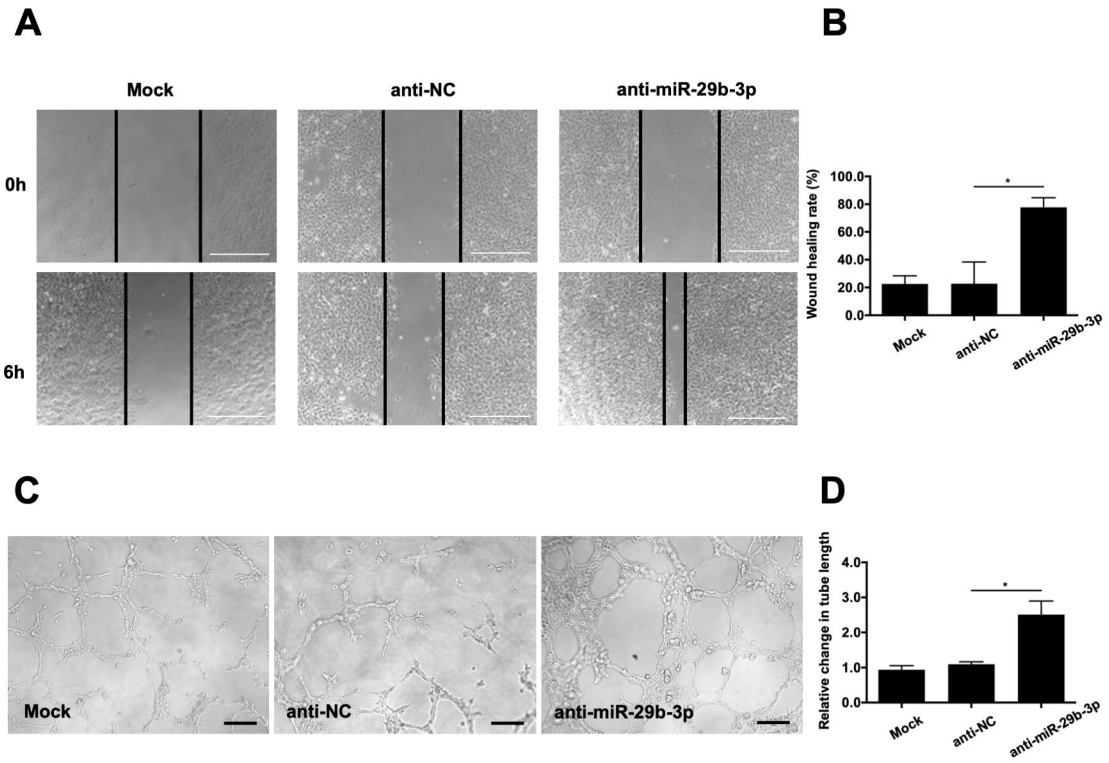

Figure 5. Effects of anti-microRNA (miR)-29b-3p on the migration and angiogenesis of RMECs. **A**: Representative images of wound scratch assays after transfecting retinal microvascular endothelial cells (RMECs) with 100 nmol/l of anti-miR-29b-3p or negative control inhibitor (anti-NC). Images were taken at 0 and 6 h after the wound layer was scratched with a pipette tip. Scale bar: 500 µm. **B**: Statistical analysis of wound healing rates in each group revealed that transfection with anti-miR-29b-3p enhanced RMEC migration compared with that of the anti-NC group. **C**: Representative images of tube formation assays at 6 h after seeding RMECs transfected with 100 nmol/l of anti-miR-29b-3p or anti-NC on Matrigel. Scale bar: 100 µm. **D**: Statistical analysis of the relative change in tube length revealed that transfection with anti-miR-29b-3p statistically significantly increased RMEC angiogenesis compared with that of the anti-NC group. The tube length was quantified by calculating the cumulative length of the tubes in each image, and the relative change was compared against the mock-transfected group. n=3 per group. *p<0.05.

and metastasis by targeting a network of factors involved in collagen remodeling, matrix degradation, and angiogenesis, including angiopoietin-like 4, lysyl oxidase, matrix metalloproteinase (MMP)-2, MMP-9, PDGF, and VEGF [17]. Additional studies have shown that miR-29b inhibits tumor angiogenesis in endometrial carcinoma by targeting VEGFA via the mitogen-activated protein kinase/extracellular-related kinase and phosphoinositide 3-kinase/Akt signaling pathways [16]. In heart tissues, it was reported that berberine promotes ischemia-induced angiogenesis by upregulating miR-29b expression [36]. Additionally, Cai et al. reported that in a model of laser-induced choroidal neovascularization, nuclear factor-κB activation inhibited miR-29s, which might contribute to angiogenesis by upregulating MMP-2 expression in retinal pigment epithelial cells [37]. Consistent with these previous studies, we found that miR-29b-3p decreased cell migratory capacity while inhibition of miR-29b-3p enhanced cell migration in RMECs. Tube formation was also impaired by upregulation of miR-29b-3p, and was increased by miR-29b inhibition. Therefore, our gain- and loss-of-function experiments have highlighted critical roles of miR-29b in angiogenesis of RMECs.

Angiogenesis is regulated by a cohort of angiogenesis-related factors, including VEGF, PDGF, FGF, and transforming growth factor [3]. VEGFA, the most prevalent member of the VEGF family, is a proangiogenic glycoprotein involved in the proliferation and migration of endothelial cells. VEGFA is also involved in vascular permeability by binding to the VEGF receptors, including VEGFR-1 and -2, as well as nucleoprotein-1 and -2 [21,38]. Recent studies revealed that miR-29b regulates the expression of VEGFA by directly binding to their 3′-UTRs [16, 17, 23, 24]. Consistent with those studies, we found that miR-29b-3p downregulated VEGFA expression, whereas inhibition of miR-29b-3p increased VEGFA expression. PDGF, originally isolated from

platelets, is a ubiquitous growth factor that stimulates cellular proliferation and directs cellular movement [22]. PDGF contributes to the recruitment of pericytes to surround newly formed vessels [5,39]. PDGFB is the predominant isoform of the PDGF family expressed in ocular tissue [40]. In addition to VEGFA, direct targeting of miR-29b to PDGFB was experimentally validated with luciferase reporter gene assays [17, 25]. Using RMECs, we found that miR-29b-3p strongly inhibited PDGFB expression while inhibition of miR-29b-3p increased PDGFB expression. Considering the mode of action of miRNAs, we think that miR-29b-3p binds to the VEGFA and PDGFB gene transcripts and degrades the target mRNAs, and thus, regulates RMEC proliferation, migration, and angiogenesis.

This study had several limitations. In particular, we cannot exclude the possibility that other unknown target sites for miR-29b are involved in its antiangiogenic effects. The

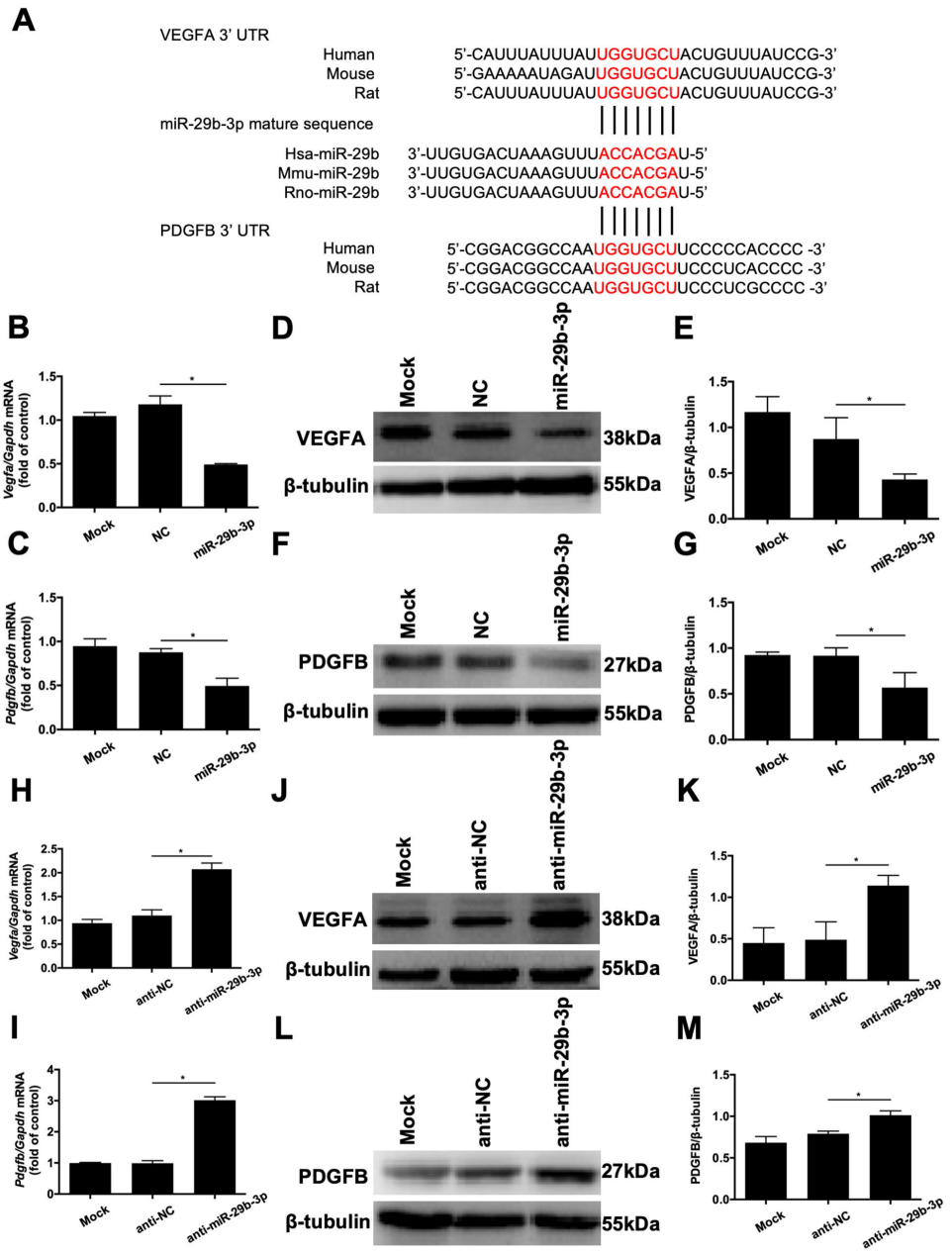

Figure 6. VEGFA and PDGFB are potential targets of microRNA (miR)-29b-3p. **A**: Bioinformatics analysis revealed that the miR-29b-3p recognition sites (shown in red) on the 3′-untranslated regions of vascular endothelial growth factor A (VEGFA) and platelet-derived growth factor B (PDGFB) are highly conserved among rat (rno-), human (hsa-), and mouse (mmu-) genes. **B**, **C**: Real-time quantitative PCR analysis revealed that transfection of retinal microvascular endothelial cells (RMECs) with miR-29b-3p statistically significantly inhibited the mRNA expression of VEGFA and PDGFB compared with that of the negative control (NC) group at 48 h after transfection. **D**–**G**: At 72 h after transfection, western blotting revealed that miR-29b-3p decreased the protein expression levels of VEGFA and PDGFB compared with those of the NC group. **H**, **I**: At 48 h after transfection, real-time quantitative PCR revealed that anti-miR-29b-3p statistically significantly increased the mRNA expression levels of VEGFA and PDGFB in RMECs compared with those of the anti-NC group. **J**–**M**: At 72 h after transfection, western blotting revealed that anti-miR-29b-3p increased the protein expression levels of VEGFA and PDGFB in RMECs compared with those of the anti-NC group. Glyceraldehyde 3-phosphate dehydrogenase (GAPDH) and β-tubulin were used as the internal controls for quantitative real-time PCR and western blotting, respectively. n=3 per group. *p<0.05.

proangiogenic effects of miR-29b should be verified in vivo using animal models in future studies.

In conclusion, this study adds to the growing body of evidence implicating miRNAs in the regulation of angiogenesis. There are several ongoing clinical trials designed to test the efficacy of miRNAs in the treatment of various disorders, such that miRNA-based gene therapy may become a novel therapeutic option for a wide range of diseases in the future [41]. Based on these data, we speculate that miR-29b-3p may become a potential therapeutic target for retinal neovascularization. This assumption requires further experiments to validate and more clinical trials to verify.

APPENDIX 1. CERTIFICATE OF ANALYSIS OF RAT RETINAL MICROVASCULAR ENDOTHELIAL CELLS.

To access the data, click or select the words "Appendix 1."

APPENDIX 2. FULL WESTERN BLOTS AS SUPPLEMENTARY FIGURES.

To access the data, click or select the words "Appendix 2."

APPENDIX 3. FULL WESTERN BLOTS AS SUPPLEMENTARY FIGURES.

To access the data, click or select the words "Appendix 3."

APPENDIX 4. FULL WESTERN BLOTS AS SUPPLEMENTARY FIGURES.

To access the data, click or select the words "Appendix 4."

APPENDIX 5. FULL WESTERN BLOTS AS SUPPLEMENTARY FIGURES.

To access the data, click or select the words "Appendix 5."

APPENDIX 6. FULL WESTERN BLOTS AS SUPPLEMENTARY FIGURES.

To access the data, click or select the words "Appendix 6."

APPENDIX 7. FULL WESTERN BLOTS AS SUPPLEMENTARY FIGURES.

To access the data, click or select the words "Appendix 7."

APPENDIX 8. FULL WESTERN BLOTS AS SUPPLEMENTARY FIGURES.

To access the data, click or select the words "Appendix 8."

APPENDIX 9. FULL WESTERN BLOTS AS SUPPLEMENTARY FIGURES.

To access the data, click or select the words "Appendix 9."

ACKNOWLEDGMENTS

This work was supported by grants from the National Key Basic Research Program of 355 China (2013CB967503), the National Natural Science Foundation of China (81570854), the Youth Project of the National Natural Science Fund (81600739, 81700861, 81700863, 81800846), Shanghai Sailing Program (16YF1401300) and Science and Technology Commission of Shanghai Municipality (16411953700). Gezhi Xu (xugezhi@sohu.com) and Jun Ma (ma886615@126.com) are both the co-corresponding authors of this work.

REFERENCES

1. Das A, McGuire PG. Retinal and choroidal angiogenesis: pathophysiology and strategies for inhibition. Prog Retin Eye Res 2003; 22:721-48. [PMID: 14575722].
2. Bharadwaj AS, Appukuttan B, Wilmarth PA, Pan Y, Stempel AJ, Chipps TJ, Benedetti EE, Zamora DO, Choi D, David LL, Smith JR. Role of the retinal vascular endothelial cell in ocular disease. Prog Retin Eye Res 2013; 32:102-80. [PMID: 22982179].
3. Yang S, Zhao J, Sun X. Resistance to anti-VEGF therapy in neovascular age-related macular degeneration: a comprehensive review. Drug Des Devel Ther 2016; 10:1857-67. [PMID: 27330279].
4. Kruger Falk M, Kemp H, Sorensen TL. Four-year treatment results of neovascular age-related macular degeneration with ranibizumab and causes for discontinuation of treatment. Am J Ophthalmol 2013; 155:89-95. PMID: 23022167
5. Abramsson A, Lindblom P, Betsholtz C. Endothelial and nonendothelial sources of PDGF-B regulate pericyte recruitment and influence vascular pattern formation in tumors. J Clin Invest 2003; 112:1142-51. [PMID: 14561699].
6. Frank RN. Growth factors in age-related macular degeneration: pathogenic and therapeutic implications. Ophthalmic Res 1997; 29:341-53. [PMID: 9323725].
7. He L, Hannon GJ. MicroRNAs: small RNAs with a big role in gene regulation. Nat Rev Genet 2004; 5:522-31. [PMID: 15211354].
8. Bartel DP. MicroRNAs: target recognition and regulatory functions. Cell 2009; 136:215-33. [PMID: 19167326].
9. Ambros V. The functions of animal microRNAs. Nature 2004; 431:350-5. [PMID: 15372042].
10. Shen J, Yang X, Xie B, Chen Y, Swaim M, Hackett SF, Campochiaro PA. MicroRNAs regulate ocular neovascularization. Mol Ther 2008; 16:1208-16. [PMID: 18500251].

11. Xu S. microRNA expression in the eyes and their significance in relation to functions. Prog Retin Eye Res 2009; 28:87-116. [PMID: 19071227].

12. Kriegel AJ, Liu Y, Fang Y, Ding X, Liang M. The miR-29 family: genomics, cell biology, and relevance to renal and cardiovascular injury. Physiol Genomics 2012; 44:237-44. [PMID: 22214600].

13. Li J, Chan MC, Yu Y, Bei Y, Chen P, Zhou Q, Cheng L, Chen L, Ziegler O, Rowe GC, Das S, Xiao J. miR-29b contributes to multiple types of muscle atrophy. Nat Commun 2017; 8:15201-[PMID: 28541289].

14. van Rooij E, Sutherland LB, Thatcher JE, DiMaio JM, Naseem RH, Marshall WS, Hill JA, Olson EN. Dysregulation of microRNAs after myocardial infarction reveals a role of miR-29 in cardiac fibrosis. Proc Natl Acad Sci USA 2008; 105:13027-32. [PMID: 18723672].

15. Kurtz CL, Peck BC, Fannin EE, Beysen C, Miao J, Landstreet SR, Ding S, Turaga V, Lund PK, Turner S, Biddinger SB, Vickers KC, Sethupathy P. MicroRNA-29 fine-tunes the expression of key FOXA2-activated lipid metabolism genes and is dysregulated in animal models of insulin resistance and diabetes. Diabetes 2014; 63:3141-8. [PMID: 24722248].

16. Chen HX, Xu XX, Tan BZ, Zhang Z, Zhou XD. MicroRNA-29b Inhibits Angiogenesis by Targeting VEGFA through the MAPK/ERK and PI3K/Akt Signaling Pathways in Endometrial Carcinoma. Cell Physiol Biochem 2017; 41:933-46. [PMID: 28222438].

17. Chou J, Lin JH, Brenot A, Kim JW, Provot S, Werb Z. GATA3 suppresses metastasis and modulates the tumour microenvironment by regulating microRNA-29b expression. Nat Cell Biol 2013; 15:201-13. [PMID: 23354167].

18. Cortez MA, Nicoloso MS, Shimizu M, Rossi S, Gopisetty G, Molina JR, Carlotti C Jr, Tirapelli D, Neder L, Brassesco MS, Scrideli CA, Tone LG, Georgescu MM, Zhang W, Puduvalli V, Calin GA. miR-29b and miR-125a regulate podoplanin and suppress invasion in glioblastoma. Genes Chromosomes Cancer 2010; 49:981-90. [PMID: 20665731].

19. Yan B, Guo Q, Fu FJ, Wang Z, Yin Z, Wei YB, Yang JR. The role of miR-29b in cancer: regulation, function, and signaling. Onco Targets Ther 2015; 8:539-48. [PMID: 25767398].

20. Scholzen T, Gerdes J. The Ki-67 protein: from the known and the unknown. J Cell Physiol 2000; 182:311-22. [PMID: 10653597].

21. Witmer AN, Vrensen GF, Van Noorden CJ, Schlingemann RO. Vascular endothelial growth factors and angiogenesis in eye disease. Prog Retin Eye Res 2003; 22:1-29. [PMID: 12597922].

22. Xue Y, Lim S, Yang Y, Wang Z, Jensen LD, Hedlund EM, Andersson P, Sasahara M, Larsson O, Galter D, Cao R, Hosaka K, Cao Y. PDGF-BB modulates hematopoiesis and tumor angiogenesis by inducing erythropoietin production in stromal cells. Nat Med 2011; 18:100-10. [PMID: 22138754].

23. Li P, Guo W, Du L, Zhao J, Wang Y, Liu L, Hu Y, Hou Y. microRNA-29b contributes to pre-eclampsia through its effects on apoptosis, invasion and angiogenesis of trophoblast cells. Clin Sci (Lond) 2013; 124:27-40. [PMID: 22716646].

24. Szczyrba J, Nolte E, Hart M, Doll C, Wach S, Taubert H, Keck B, Kremmer E, Stohr R, Hartmann A, Wieland W, Wullich B, Grasser FA. Identification of ZNF217, hnRNP-K, VEGF-A and IPO7 as targets for microRNAs that are downregulated in prostate carcinoma. Int J Cancer 2013; 132:775-84. [PMID: 22815235].

25. Hu G, Yao H, Chaudhuri AD, Duan M, Yelamanchili SV, Wen H, Cheney PD, Fox HS, Buch S. Exosome-mediated shuttling of microRNA-29 regulates HIV Tat and morphine-mediated neuronal dysfunction. Cell Death Dis 2012; 3:e381-[PMID: 22932723].

26. Chen S, Wang LL, Sun KX, Liu Y, Guan X, Zong ZH, Zhao Y. LncRNA TDRG1 enhances tumorigenicity in endometrial carcinoma by binding and targeting VEGF-A protein. Biochim Biophys Acta Mol Basis Dis 2018; 1864:9 Pt B3013-21. [PMID: 29920344].

27. Garzon R, Heaphy CE, Havelange V, Fabbri M, Volinia S, Tsao T, Zanesi N, Kornblau SM, Marcucci G, Calin GA, Andreeff M, Croce CM. MicroRNA 29b functions in acute myeloid leukemia. Blood 2009; 114:5331-41. [PMID: 19850741].

28. Iorio MV, Ferracin M, Liu CG, Veronese A, Spizzo R, Sabbioni S, Magri E, Pedriali M, Fabbri M, Campiglio M, Menard S, Palazzo JP, Rosenberg A, Musiani P, Volinia S, Nenci I, Calin GA, Querzoli P, Negrini M, Croce CM. MicroRNA gene expression deregulation in human breast cancer. Cancer Res 2005; 65:7065-70. [PMID: 16103053].

29. Yanaihara N, Caplen N, Bowman E, Seike M, Kumamoto K, Yi M, Stephens RM, Okamoto A, Yokota J, Tanaka T, Calin GA, Liu CG, Croce CM, Harris CC. Unique microRNA molecular profiles in lung cancer diagnosis and prognosis. Cancer Cell 2006; 9:189-98. [PMID: 16530703].

30. Mott JL, Kobayashi S, Bronk SF, Gores GJ. mir-29 regulates Mcl-1 protein expression and apoptosis. Oncogene 2007; 26:6133-40. [PMID: 17404574].

31. Fabbri M, Garzon R, Cimmino A, Liu Z, Zanesi N, Callegari E, Liu S, Alder H, Costinean S, Fernandez-Cymering C, Volinia S, Guler G, Morrison CD, Chan KK, Marcucci G, Calin GA, Huebner K, Croce CM. MicroRNA-29 family reverts aberrant methylation in lung cancer by targeting DNA methyltransferases 3A and 3B. Proc Natl Acad Sci USA 2007; 104:15805-10. [PMID: 17890317].

32. Ding DP, Chen ZL, Zhao XH, Wang JW, Sun J, Wang Z, Tan FW, Tan XG, Li BZ, Zhou F, Shao K, Li N, Qiu B, He J. miR-29c induces cell cycle arrest in esophageal squamous cell carcinoma by modulating cyclin E expression. Carcinogenesis 2011; 32:1025-32. [PMID: 21551130].

33. Bendris N, Loukil A, Cheung C, Arsic N, Rebouissou C, Hipskind R, Peter M, Lemmers B, Blanchard JM. Cyclin A2: a genuine cell cycle regulator? Biomol Concepts 2012; 3:535-43. [PMID: 25436557].

34. Ohtsubo M, Theodoras AM, Schumacher J, Roberts JM, Pagano M. Human cyclin E, a nuclear protein essential for the

G1-to-S phase transition. Mol Cell Biol 1995; 15:2612-24. [PMID: 7739542].

35. Casimiro MC, Velasco-Velazquez M, Aguirre-Alvarado C, Pestell RG. Overview of cyclins D1 function in cancer and the CDK inhibitor landscape: past and present. Expert Opin Investig Drugs 2014; 23:295-304. [PMID: 24387133].

36. Zhu ML, Yin YL, Ping S, Yu HY, Wan GR, Jian X, Li P. Berberine promotes ischemia-induced angiogenesis in mice heart via upregulation of microRNA-29b. Clin Exp Hypertens 2017; 39:672-9. [PMID: 28722488].

37. Cai J, Yin G, Lin B, Wang X, Liu X, Chen X, Yan D, Shan G, Qu J, Wu S. Roles of NFkappaB-miR-29s-MMP-2 circuitry in experimental choroidal neovascularization. J Neuroinflammation 2014; 11:88-[PMID: 24886609].

38. Otrock ZK, Makarem JA, Shamseddine AI. Vascular endothelial growth factor family of ligands and receptors Blood Cells Mol Dis 2007; 38:258-68. review[PMID: 17344076].

39. Hellstrom M, Kalen M, Lindahl P, Abramsson A, Betsholtz C. Role of PDGF-B and PDGFR-beta in recruitment of vascular smooth muscle cells and pericytes during embryonic blood vessel formation in the mouse. Development 1999; 126:3047-55. [PMID: 10375497].

40. Siedlecki J, Wertheimer C, Wolf A, Liegl R, Priglinger C, Priglinger S, Eibl-Lindner K. Combined VEGF and PDGF inhibition for neovascular AMD: anti-angiogenic properties of axitinib on human endothelial cells and pericytes in vitro. Graefes Arch Clin Exp Ophthalmol 2017; 255:963-72. [PMID: 28161830].

41. Simonson B, Das S. MicroRNA Therapeutics: the Next Magic Bullet? Mini Rev Med Chem 2015; 15:467-74. [PMID: 25807941].

Articles are provided courtesy of Emory University and the Zhongshan Ophthalmic Center, Sun Yat-sen University, P.R. China. The print version of this article was created on 24 February 2020. This reflects all typographical corrections and errata to the article through that date. Details of any changes may be found in the online version of the article.